Ozone production in the upper troposphere and the influence of aircraft during SONEX: Approach of NO_x-saturated conditions

L. Jaeglé,[1] D.J. Jacob,[1] W.H. Brune,[2] I.C. Faloona,[2] D. Tan,[2] Y. Kondo,[3] G.W. Sachse,[4] B. Anderson,[4] G.L. Gregory,[4] S. Vay,[4] H.B. Singh,[5] D.R. Blake,[6] R. Shetter[7]

Abstract. During October/November 1997, simultaneous observations of NO, HO_2 and other species were obtained as part of the SONEX campaign in the upper troposphere. We use these observations, over the North Atlantic (40-60°N), to derive ozone production rates, $P(O_3)$, and to examine the relationship between $P(O_3)$ and the concentrations of NO_x (= NO + NO_2) and HO_x (= OH + peroxy) radicals. A positive correlation is found between $P(O_3)$ and NO_x over the entire data set, which reflects the association of elevated HO_x with elevated NO_x injected by deep convection and lightning. By filtering out this association we find that for NO_x>70 pptv, $P(O_3)$ is nearly independent of NO_x, showing the approach of NO_x-saturated conditions. Predicted doubling of aircraft emissions in the future will result in less than doubling of the aircraft contribution to ozone over the North Atlantic in the fall. Greater sensitivity to aircraft emissions would be expected in the summer.

Introduction

In recent years, considerable attention has been given to the potential role of aircraft emissions of nitrogen oxides (NO_x = NO + NO_2) on the concentration of upper tropospheric ozone, an effective greenhouse gas [*NASA*, 1997]. Ozone is produced in the troposphere by the photochemical oxidation of CO and hydrocarbons which is catalyzed by NO_x radicals and hydrogen oxide radicals (HO_x = OH + peroxy). Oxidation of CO dominates in the upper troposphere, and the rate-limiting step for ozone production is the reaction of HO_2 with NO (R2):

$$CO + OH (+ O_2) \rightarrow CO_2 + HO_2 \quad (R1)$$

$$HO_2 + NO \rightarrow OH + NO_2 \quad (R2)$$

$$NO_2 + h\nu (+ O_2) \rightarrow NO + O_3 \quad (R3)$$

The sensitivity of the ozone production rate, $P(O_3)$, to increasing NO_x is critical to the assessment of aircraft effects. Photochemical models [e.g., *Brasseur et al.*, 1996] predict that $P(O_3)$ should increase with increasing NO_x (NO_x-limited regime) up to a turnover point of a few hundred pptv NO_x, beyond which further increases in NO_x cause $P(O_3)$ to decrease (NO_x-saturated regime). These two regimes result from the dual role of NO_x in regulating the chemistry of HO_x radicals. On the one hand, NO_x drives the ozone production cycle (R1)-(R3). On the other hand, NO_x promotes the removal of HO_x through reactions of OH with HO_2, HNO_4, and NO_2 [*Wennberg et al.*, 1998]. The chemical regime for ozone production is largely determined by the relative magnitudes of the sources of HO_x and NO_x [*Jaeglé et al.*, 1998].

Ozone production rates in the upper troposphere have been previously determined from simultaneous measurements of HO_2 and NO during three recent aircraft campaigns: ASHOE/MAESA, STRAT and SUCCESS [*Folkins et al.*, 1997; *Wennberg et al.*, 1998; *Brune et al.*, 1998; *Jaeglé et al.*, 1998]. Examination of the $P(O_3)$ versus NO_x relationships indicated a much greater prevalence for NO_x-limited conditions than expected from models [*Folkins et al.*, 1997; *Jaeglé et al.*, 1998]. However, as we will see, interpretation of this relationship in terms of the chemical regime for ozone production can be biased by a commonality of sources for NO_x and HO_x.

We present here the first direct evidence of NO_x-saturated conditions for ozone production in the upper troposphere and show that a simple interpretation of the observed $P(O_3)$ versus NO_x relationship as a partial derivative $\partial P(O_3)/\partial NO_x$ overestimates the actual sensitivity of ozone concentrations to emissions from aircraft. We use concurrent observations of HO_2 and NO obtained during the Subsonic assessment: Ozone and NO_x Experiment (SONEX) DC-8 aircraft campaign. SONEX took place in October and November 1997 in the North Atlantic flight corridor, a region of dense aircraft traffic in the upper troposphere [*Singh et al.*, this issue]. Companion papers use the SONEX data to improve our understanding of the chemistry and sources of NO_x [*Kondo et al.*, this issue; *Thompson et al.*, this issue], and HO_x [*Brune et al.*, this issue].

Calculation of ozone production

Singh et al. [this issue] describe the flight tracks and the instruments aboard the DC-8 aircraft during SONEX. We focus here on observations made in the upper troposphere (8-12 km) between 40 and 60°N latitude, the main theater of operations. We exclude observations made in clouds (diagnosed by an abundance of particles larger than 3 μm), in fresh aircraft exhaust plumes (short duration peaks of elevated NO_x and condensation nuclei), at high solar zenith angles (>80°), and in air masses with stratospheric influence (O_3>90 ppbv and CH_4<1760 ppbv).

We define the budget of ozone as that of the odd-oxygen family, O_x (O_x=O_3 + O + $O(^1D)$ + NO_2 + HNO_4 + HNO_3 + 2NO_3+ 3N_2O_5), to account for rapid chemical cycling within this family. Ozone typically accounts for over 99% of O_x, so the budgets of ozone and O_x can be viewed as equivalent. In addition to reaction (R2), ozone can be produced by the reaction of organic peroxy radicals, RO_2, with NO,

$$RO_2 + NO \rightarrow RO + NO_2 . \quad (R4)$$

Ozone chemical loss is almost exclusively due to:

$$O_3 + HO_2 \rightarrow OH + 2\ O_2 \quad (R5)$$

$$O_3 + OH \rightarrow HO_2 + O_2 \quad (R6)$$

$$O(^1D) + H_2O \rightarrow 2\ OH \quad (R7)$$

$$N_2O_5 + \text{aerosols} \rightarrow 2\ HNO_3 . \quad (R8)$$

The ozone production and loss rates, $P(O_3)$ and $L(O_3)$, can thus be expressed as:

$$P(O_3) = k_2[HO_2][NO] + k_4[RO_2][NO] \quad (1)$$

[1]Harvard University, Cambridge, Massachusetts.
[2]Pennsylvania State University, University Park.
[3]Nagoya University, Japan.
[4]NASA Langley Research Center, Hampton, Virginia.
[5]NASA Ames Research Center, Moffett Field, California.
[6]University of California, Irvine, California.
[7]National Center for Atmospheric Research, Boulder, Colorado.

$$L(O_3) = k_5[O_3][HO_2] + k_6[O_3][OH] + k_7[O(^1D)][H_2O] + k_8[N_2O_5], \quad (2)$$

where k_i is the rate constant for reaction (Ri), and k_4 is weighted over the different RO_2 radicals contributing to ozone production. In the above expressions, we neglect the role of HNO_3+OH, which is a minor source of ozone (as per our definition of the O_x chemical family).

We use equations (1) and (2) with 1-minute averages of concurrent observations of NO, HO_2, OH, H_2O, O_3, UV actinic flux, aerosol surface area, temperature and pressure, to calculate instantaneous values of $P(O_3)$ and $L(O_3)$ along the flight tracks of the DC-8. For species which are not observed (RO_2, $O(^1D)$, N_2O_5) we use calculations from a diel steady state model [*Jaeglé et al.*, 1998] constrained with local observations of O_3, H_2O, NO, HNO_3, PAN, acetone, CO, CH_4, C_2H_6, C_3H_8, C_4 alkanes, UV actinic flux, aerosol surface area, temperature and pressure. The resulting instantaneous $P(O_3)$ and $L(O_3)$ rates are then scaled to 24-hour average values by using local results from the diel steady state model:

$$<Rate_{obs}>_{24h} = Rate_{obs}(t) \times <Rate_{model}>_{24h}/Rate_{model}(t), \quad (3)$$

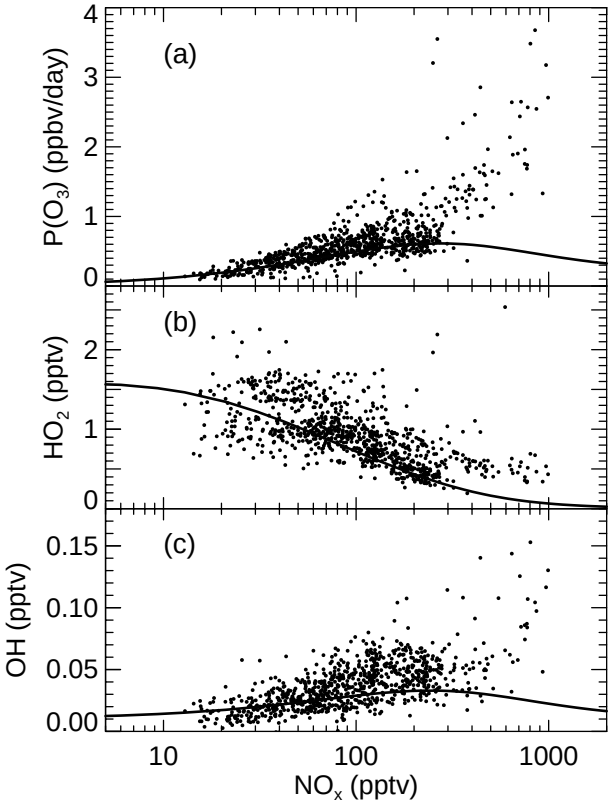

Figure 1. Observed ozone production rates $P(O_3)$, and concentrations of HO_2 and OH in SONEX (8-12 km altitude, 40-60ºN latitude) plotted as a function of the NO_x concentration (NO_x = observed NO + modeled NO_2). The observed rates and concentrations are averaged over 24 hours, using diel factors obtained from a locally constrained photochemical model. The lines on the three panels correspond to model-calculated values for median upper tropospheric background conditions during SONEX (see text).

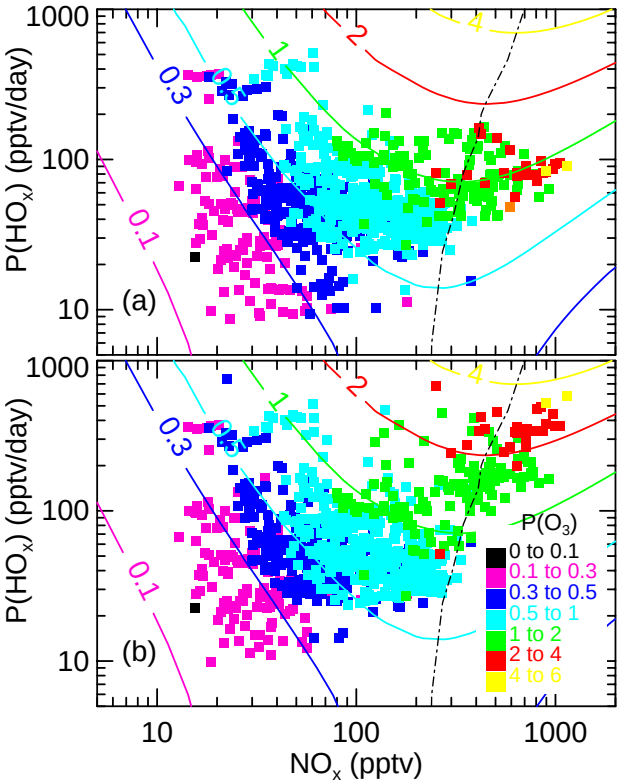

Figure 2. Ozone production rate $P(O_3)$ (ppbv/day) in SONEX as a function of NO_x mixing ratio and the primary HO_x source, $P(HO_x)$, in the upper troposphere (8-12 km). The contour lines correspond to model calculations of 24-hour average $P(O_3)$ for background conditions during SONEX. Values of $P(O_3)$ computed from observed NO and HO_2 and scaled to 24-hour averages (see Figure 1) are shown as color-coded squares. In panel a, the values of $P(HO_x)$ corresponding to the observed $P(O_3)$ are calculated using the observed concentrations of H_2O and acetone. In panel b, $P(HO_x)$ was increased in order to match the observations of HO_2 where required (see text). The dashed line corresponds to $\partial P(O_3)/\partial NO_x=0$.

A more detailed description of the model as applied to SONEX observations can be found in *Jaeglé et al.* [Photochemistry of HO_x in the upper troposphere at northern midlatitudes, *submitted to J. Geophys. Res.*, 1999, hereafter referred to as *J99*].

Relationships between NO_x, HO_x, and ozone production

Figure 1a shows the relationship between the 24-hour average values of $P(O_3)$ derived from observed HO_2 and NO, and the local NO_x concentrations in the upper troposphere (8-12 km) between 40ºN and 60ºN latitude. The calculated median $P(O_3)$ for SONEX was 0.57 ppbv/day. The median $L(O_3)$ was 0.13 ppbv/day (not shown here), resulting in a net ozone production of 0.44 ppbv/day. Reaction of NO with HO_2 dominates ozone production; reaction (R4) contributes on average less than 15% of the total $P(O_3)$. Reactions of O_3 with HO_2 and OH contribute more than 80% of $L(O_3)$, while reactions (R7) and (R8) contribute 10% and 5% respectively.

The line in Figure 1a shows the expected dependence of ozone production on NO_x, for diel steady state model calculations where model input variables are specified from median background conditions observed during SONEX at 10 km [*J99*]: 55 ppbv O_3, 120 ppmv H_2O, 120 pptv HNO_3, 64 pptv PAN, 510 pptv acetone, 90 ppbv CO, 1761 ppbv CH_4, 670 pptv C_2H_6, 79 pptv C_3H_8, 55

pptv C_4 alkanes, 50ºN latitude, 285 DU ozone column, 8 $\mu m^2 cm^{-3}$ aerosol surface area, 227 K temperature, on November 1. In the model, $P(O_3)$ becomes relatively independent of NO_x above 70 pptv; and the turnover to the NO_x-saturated regime ($\partial P(O_3)/\partial NO_x=0$) takes place at 300 pptv. The bulk of the observations (NO_x<300 pptv) shows indeed a leveling off of the dependence of $P(O_3)$ on NO_x as NO_x increases above 70 pptv, in accordance with the expected behavior. However, for the highest NO_x concentrations, the values of $P(O_3)$ computed from observed HO_2 and NO continue to increase with increasing NO_x, suggesting a consistently NO_x-limited regime which is at odds with model results.

The largest NO_x concentrations (>300 pptv) shown in Figure 1 correspond to relatively fresh convective outflows sampled close to the U.S. East coast [*Thompson et al.*, this issue]. Elevated NO_x/NO_y ratios (>0.5 mol/mol), backtrajectory calculations and satellite lightning imagery all support a strong source of NO_x from lightning associated with this convection [*Pickering et al.*, 1999]. These air masses were also characterized by an enhanced HO_x source resulting from convective transport of surface air with elevated concentrations of HO_x precursors such as peroxides and CH_2O [*J99*]. Based on (1), comparison between observed and modeled $P(O_3)$ for a given NO_x concentration is roughly equivalent to comparison of observed and modeled HO_2 concentrations. We see from Figure 1b that the model constrained with background conditions for SONEX underestimates HO_2 by a factor of two or more when NO_x>300 pptv. Using the locally observed concentrations of HO_x precursors (H_2O, acetone, peroxides and CH_2O) for these high-NO_x points improves the agreement but still comes short of the observed levels. The discrepancy suggests the presence of other unmeasured sources, such as higher aldehydes, possibly also resulting from convection [*Müller and Brasseur*, 1999]. It could also reflect flaws in our understanding of HO_x chemistry in the high-NO_x regime [*Faloona et al.*, 1999], or other unknown HO_x sources [*Chatfield et al*., 1999]. For the remaining observations (NO_x<300 pptv), the dependence of HO_2 and OH on NO_x is generally well reproduced (Fig. 1b and 1c). The scatter around the model lines in Figure 1 can be explained by variations in the magnitude of the local HO_x sources [*J99*].

In models of the upper troposphere, $P(O_3)$ is largely determined by two variables: NO_x mixing ratios and the strength of the primary HO_x source, $P(HO_x)$ [*Jaeglé et al.*, 1998]. Figure 2 shows the variations of $P(O_3)$ as a function of NO_x and $P(HO_x)$. We separate *primary* sources (i.e. sources independent of HO_x) from *secondary* sources (i.e. sources dependent on a preexisting pool of HO_x), and define the primary HO_x source as:

$$P(HO_x) = 2k_7[O(^1D)][H_2O] + y_{acet}J_{acet}[\text{Acetone}] + \sum_i y_{Xi}J_{Xi}[X_i], \quad (4)$$

where J_{acet} and y_{acet} are the photolysis rate constant and HO_x yield for acetone, and J_{Xi} and y_{Xi} are the photolysis rate constants and HO_x yields for other convected HO_x precursors such as peroxides and aldehydes (see *Müller and Brasseur* [1999] for this definition of the primary HO_x source). The value of y_{acet} is about three [*Singh et al.*, 1995]. Methane oxidation by OH, and the subsequent photolysis of CH_2O was an important HO_x source during SONEX [*J99*]. We do not include this source in our definition of $P(HO_x)$ because it is a secondary HO_x source.

In Figure 2a, we calculate $P(HO_x)$ based on the observed H_2O and acetone. $P(HO_x)$ is averaged over 24 hours using (3). In Figure 2b, in addition to H_2O and acetone, we include an additional HO_x source ($\Sigma y_{Xi}J_{Xi}[X_i]$) as required to match the observed HO_2 concentrations. This source might include contributions from convected peroxides and aldehydes, which we cannot easily quantify from our model. Its impact on $P(HO_x)$ is small (less than 50%) except for observations in continental convective outflows with elevated NO_x (15% of the points in Figure 2b). As seen in Figure 2, model calculations of $P(O_3)$ for median background SONEX conditions with varying NO_x and $P(HO_x)$ (contour lines) generally reproduce the observations (square symbols).

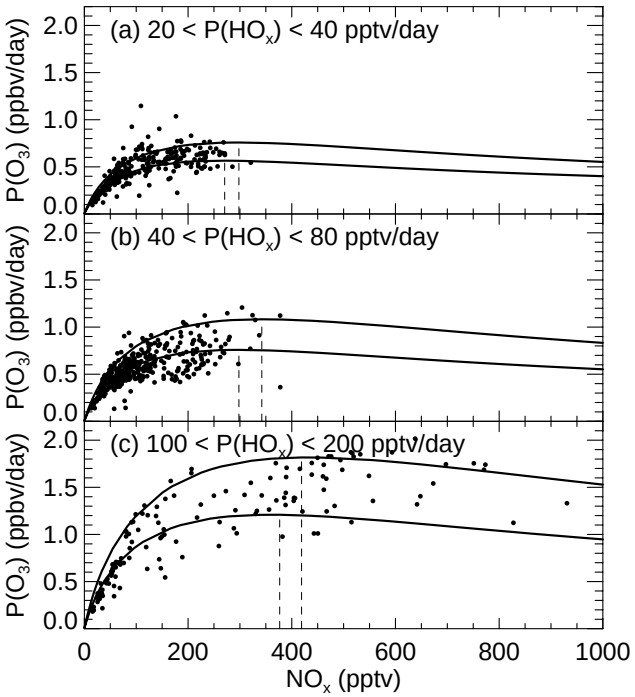

Figure 3. Observed ozone production rate in SONEX (24-hour average) as a function of NO_x mixing ratios for three ranges of the primary HO_x production $P(HO_x)$: (a) 20-40 pptv/day, (b) 40-80 pptv/day, (c) 100-200 pptv/day. Model calculations corresponding to the limits of each range are also shown. Note the linear scale for NO_x. The dashed lines correspond to $\partial P(O_3)/\partial NO_x=0$.

The primary HO_x source in the SONEX data displays large variations, with 24-hour average values ranging from 10 pptv/day to 700 pptv/day (Fig. 2). Elevated $P(HO_x)$ values (200-700 pptv/day) are sometimes associated with low NO_x concentrations (<30-40 pptv). These air masses were influenced by recent marine convection and high concentrations of water vapor; despite the enhanced source of HO_x, the low levels of NO_x result in relatively low $P(O_3)$ (0.1-0.5 ppbv/day). Elevated $P(HO_x)$ is also found in association with high NO_x concentrations (>300 pptv). As noted above, the elevated NO_x was the result of recent lightning and convection, and concurrent enhancement of $P(HO_x)$ would be expected from the convective injection of HO_x precursors. The positive correlation between high NO_x and $P(HO_x)$ in the observations is particularly apparent in Figure 2b, but can also be seen in Figure 2a. This correlation results in the highest levels of $P(O_3)$ observed. By supplying HO_x precursors together with NO_x, deep convection extends the NO_x-limited regime to higher concentrations of NO_x.

Chemical regime for ozone production

To diagnose the actual dependence of $P(O_3)$ on NO_x in the SONEX observations, the additional sensitivity to $P(HO_x)$ must be resolved. We therefore examined the dependence of $P(O_3)$ on NO_x for similar primary HO_x production rates. Figure 3 illustrates this

dependence for three ranges of $P(HO_x)$. The $P(HO_x)$ values used to segregate the observations are those required in order to match the observed HO_2 (Fig. 2b). Choosing instead the $P(HO_x)$ values computed from H_2O and acetone only (Fig. 2a) results in some small differences in Figure 3c.

Figure 3 shows that $P(O_3)$ derived from observations increases nearly linearly with NO_x for NO_x<70 pptv. In Figures 3a and 3b, $P(O_3)$ shows very little dependence on NO_x between 70 pptv and 300 pptv, approaching the NO_x-saturated regime. The bin with the highest levels of $P(HO_x)$ (Fig. 3c), shows a positive dependence of $P(O_3)$ on NO_x extending to a higher NO_x concentration (200 pptv) but there is still clear evidence of NO_x-saturated conditions beyond this. The median NO_x mixing ratio was 93 pptv in the upper troposphere (8-12 km) during SONEX, and the median $P(HO_x)$ was 50 pptv/day. These conditions correspond to a regime where ozone production is less sensitive to changes in NO_x.

Because of the slow photochemistry in October-November and the elevated levels of NO_x, the conditions during SONEX allowed extensive sampling of the transition region between the NO_x-limited and NO_x-saturated regimes as illustrated in Figure 3. Previous aircraft campaigns (ASHOE/MAESA, STRAT, SUCCESS), where ozone production was consistently NO_x-limited, featured lower NO_x concentrations and more active photochemistry. In the tropical upper troposphere during STRAT, NO_x mixing ratios were generally less than 100 pptv [*Wennberg et al.*, 1998]. Over the central United States during SUCCESS, springtime conditions resulted in more rapid photochemistry compared to SONEX and thus a higher transition from NO_x-limited to NO_x-saturated regimes (NO_x~500 pptv) [*Jaeglé et al.*, 1998].

Delineation of the regimes for ozone production is critical when assessing the effect of aircraft emissions. Aircraft, unlike deep convection and lightning, inject NO_x into the upper troposphere without injecting HO_x precursors (the aircraft sources of H_2O and HONO are negligibly small [*NASA*, 1997]). As summarized in *Singh et al.* [this issue], aircraft emissions might have contributed 20-70% of the observed NO_x in the upper troposphere during SONEX. A 40% aircraft effect corresponds to a 37 pptv contribution to the median observed NO_x concentration of 93 pptv. Based on the dependence shown in Figure 3b, and assuming a SONEX median value for $P(HO_x)$ of 50 pptv/day, such a NO_x increase results in an increase of $P(O_3)$ from 0.45 to 0.6 ppbv/day. For a 2-week residence time of air in the upper troposphere at midlatitudes, this increase of 0.15 ppbv/day adds about 2.1 ppbv of ozone, resulting in a 4% increase in upper tropospheric ozone in the north Atlantic flight corridor in the fall. For a larger range of $P(HO_x)$ values (20-100 pptv/day), the increase in ozone is 2-6%.

A further doubling of NO_x concentrations due to future aircraft emissions (NO_x=93+37 pptv) would only result in an additional 0.1 ppbv/day ozone production under SONEX conditions (northern midlatitudes in the fall) because of the NO_x-saturated regime. However, if the primary source of HO_x were to rise in the future, $P(O_3)$ would become more sensitive to increases in NO_x from aircraft emissions. As noted above, during summer the transition to NO_x-saturated regime occurs at higher levels of NO_x, and thus increases in aircraft emissions should continue to result in O_3 increases in the foreseeable future [*NASA*, 1997].

Conclusions

We computed ozone production rates $P(O_3)$ in the upper troposphere at northern midlatitudes, using simultaneous observations of HO_2 and NO during SONEX (October-November 1997). High levels of NO_x due to lightning and convection were associated with high concentrations of HO_x precursors also supplied by convection. The observed correlation between elevated NO_x and HO_x sources resulted in a positive relationship between $P(O_3)$ and NO_x extending over the full range of NO_x concentrations observed (up to 1 ppbv). By segregating the data according to the primary HO_x production rate, $P(HO_x)$, we find that ozone production in fact approached NO_x-saturated conditions for NO_x concentrations larger than 70 pptv. This result implies little sensitivity of $P(O_3)$ to future increases in NO_x emissions from aircraft (which unlike convective injection are not associated with a large source of HO_x) during the fall at northern midlatitudes. A greater sensitivity of $P(O_3)$ to NO_x would be expected under summer conditions.

Acknowledgments. This work was supported by the Subsonic Assessment Program (SASS) of the National Aeronautics and Space Administration (NASA).

References

Brasseur, G., J.-F. Müller, and C. Granier, Atmospheric impact of NO_x emissions by subsonic aircraft: a three-dimensional model study, *J. Geophys. Res.*, *101*, 1423-1428, 1996.

Brune, W.H., et al., Airborne in-situ OH and HO_2 observations in the cloud-free troposphere and lower stratosphere during SUCCESS, *Geophys. Res. Lett.*, *25*, 1701-1704, 1998.

Brune, W.H., et al., OH and HO_2 chemistry in the North Atlantic free troposphere, *Geophys. Res. Lett.*, this issue, 1999.

Chatfield, R.B., et al., Attributing sources for NO_x observed in the Atlantic free troposphere during the SONEX period: models and observations emphasize effects of aircraft, *submitted to J. Geophys. Res.*, 1999.

Faloona, I., et al., Observation of HO_x and its relationship with NO_x in the upper troposphere during SONEX, *submitted to J. Geophys. Res.*, 1999.

Folkins, I., et al., OH and HO_2 in two biomass burning plumes: source of HO_x and implications for ozone production, *Geophys. Res. Lett.*, *24*, 3185-3188, 1997.

Jaeglé, L., et al., Sources of HO_x and production of ozone in the upper troposphere over the United States, *Geophys. Res. Lett.*, *25*, 1705-1708, 1998

Kondo, Y., et al., Impact of aircraft emissions on NO_x in the lowermost stratosphere at northern midlatitudes, *Geophys. Res. Lett.*, this issue, 1999.

Müller, J.-F., and G. Brasseur, Sources of upper tropospheric HO_x: A three-dimensional study, *J. Geophys. Res.*, *104*, 1705-1715, 1999.

Pickering, K.E., et al., Comparison and interpretation of chemical measurements from two SONEX flights over the Canadian maritime: Lightning, convection and aircraft signatures, *submitted to J. Geophys. Res.*, 1999.

National Aeronautics and Space Administration, Atmospheric effects of aviation, *Interim assessment report of the advanced subsonic technology program*, Ref. Publ. 1400, 1997.

Singh, H.B., et al., High concentrations and photochemical fate of oxygenated hydrocarbons in the global troposphere, *Nature*, *378*, 50-54, 1995.

Singh, H.B., A.M. Thompson, and H. Schlager, SONEX airborne mission and coordinated POLINAT-2 activity: Overview and accomplishments, *Geophys. Res. Lett.*, this issue, 1999.

Thompson, A.M., et al., Fingerprinting NO_x in SONEX: What was the aircraft contribution to NO sources? *Geophys. Res. Lett.*, this issue, 1999.

Wennberg, P.O., et al., Hydrogen radicals, nitrogen radicals and the production of ozone in the middle and upper troposphere, *Science*, *279*, 49-53, 1998.

D. Blake, Department of Chemistry, University of California, Irvine, CA 92717.

W. Brune, I. Faloona, D. Tan, Pennsylvania State University, Department of Meteorology, University Park, PA 16802.

D. Jacob, L. Jaeglé (corresponding author), Division of Engineering and Applied Sciences, and Department of Earth and Planetary Sciences, Harvard University, 29 Oxford Street, Pierce Hall, Cambridge, MA 02138. (e-mail: lyj@io.harvard.edu)

Y. Kondo, Solar Terrestrial Environment Laboratory, Nagoya University, Japan.

G. Sachse, B. Anderson, G. Gregory, S. Vay, NASA Langley Research Center, Hampton, VA 23665.

R. Shetter, National Center for Atmospheric Research, Boulder, CO 80307.

H. Singh, NASA Ames Research Center, Moffett Field, CA 94035.

(Received March 8, 1999; revised May 13, 1999;
accepted May 14, 1999)